Stem Cell Research (2010) **5**, 76–89

available at www.sciencedirect.com

ScienceDirect

www.elsevier.com/locate/scr

REGULAR ARTICLE

Different stages of pluripotency determine distinct patterns of proliferation, metabolism, and lineage commitment of embryonic stem cells under hypoxia

Tiago G. Fernandes, Maria Margarida Diogo, Ana Fernandes-Platzgummer, Cláudia Lobato da Silva, Joaquim M.S. Cabral*

Institute for Biotechnology and Bioengineering (IBB), Centre for Biological and Chemical Engineering, Instituto Superior Técnico, Av. Rovisco Pais, 1049-001 Lisboa, Portugal

Received 15 October 2009; received in revised form 14 April 2010; accepted 14 April 2010

Abstract Oxygen tension is an important component of the stem cell microenvironment. Herein, we have studied the effect of low oxygen levels (2% O_2), or hypoxia, in the expansion of mouse embryonic stem (ES) cells. In the presence of leukemia inhibitory factor (LIF), cell proliferation was reduced under hypoxia and a simultaneous reduction in cell viability was also observed. Morphological changes and different cell cycle patterns were observed, suggesting some early differentiation under hypoxic conditions. However, when cells were maintained in a ground state of pluripotency, by inhibition of autocrine FGF4/ERK and GSK3 signaling, hypoxia did not affect cell proliferation, and did not induce early differentiation. As expected, there was an increase in lactate-specific production rate and a significant increase in the glucose consumption under hypoxic conditions. Nevertheless, during neural commitment, low oxygen tension exerted a positive effect on early differentiation of ground-state ES cells, resulting in a faster commitment toward neural progenitors. Overall our results demonstrate the need to specifically regulate the oxygen content, especially hypoxia, along with other culture conditions, when developing new strategies for ES cell expansion and/or controlled differentiation.

Introduction

Stem cells possess the ability for unlimited or prolonged self-renewal and to differentiate into highly distinct cell lineages. In particular, pluripotent embryonic stem (ES) cells can give rise to cells derived from the three embryonic germ layers (ectoderm, endoderm, and mesoderm) (Smith, 2001), which makes them attractive for a wide range of clinical and pharmacological applications (Klimanskaya et al., 2008; Pouton and Haynes, 2005). However, a better understanding of the mechanisms that control the expansion and differentiation of ES cells is of great importance for the systematic production of cells for therapeutic applications (Kirouac and Zandstra, 2008). Interestingly, the oxygen tensions to which cells are exposed during development are substantially lower than atmospheric levels (Jauniaux et al., 2003; Lee et al., 2001), making O_2 content a potentially important parameter when designing new strategies for stem cell expansion and/or controlled differentiation.

Mouse ES cells, in particular, can be maintained in culture in an undifferentiated state in the presence of leukemia inhibitory factor (LIF) and serum, or under serum-free

* Corresponding author. Fax: +351 21 841 90 62.
E-mail address: joaquim.cabral@ist.utl.pt (J.M.S. Cabral).

1873-5061/$ – see front matter © 2010 Elsevier B.V. All rights reserved.
doi:10.1016/j.scr.2010.04.003

conditions with LIF and bone morphogenetic protein (BMP-4) (Ying et al., 2003a). However, recent evidence has highlighted the existence of metastable pluripotent states, demonstrating that ES cells can assume distinct states of pluripotency *in vitro* (Hanna et al., 2009). Therefore, two stages of pluripotency can be defined: a naïve or ground state, and a primed or committed state of pluripotency (Nichols and Smith, 2009). Culture conditions for the maintenance of ground-state ES cells were developed and involve the utilization of small-molecule inhibitors of fibroblast growth factor (FGF)/extracellular signal-regulated kinases (ERK) and glycogen synthase kinase-3 (GSK3) signaling (Ying et al., 2008). Auto-inductive FGF4/ERK signaling poises ES cells susceptible for lineage commitment, and cells enter into a primed pluripotent state (Silva and Smith, 2008). Thus, inhibition of ERK signaling, augmented by inhibition of GSK3 to restore cellular growth and viability, allows the propagation of naïve pluripotent ES cells.

The influence of oxygen levels on this dynamic regulatory mechanism has not yet been studied, and may potentially provide new insights into ES cell proliferation, metabolism, and phenotype retention. Furthermore, in the absence of serum, elimination of inductive signals for alternative fates renders ES cells to develop efficiently into neural precursors, as the result of autocrine FGF signaling (Ying et al., 2003b). It has also been suggested that culture under low oxygen tensions allows spontaneous ES cell differentiation (Kurosawa et al., 2006), and recent evidence has revealed that reduced oxygen tensions are beneficial for the proliferation and differentiation of fetal and postnatal neural stem cells (Morrison et al., 2000; Pistollato et al., 2007). Thus, oxygen tension control during neural commitment of ground-state ES cells could potentially be used for improved efficiency in the generation of ES cell-derived neural progenitors.

The influence of low oxygen levels (2%) on the proliferation and neural differentiation of ground-state embryonic stem cells was evaluated in this work. A comprehensive analysis of ground-state ES cell proliferation kinetics, cell viability, expression of pluripotency markers, cell cycle, and metabolic profile was performed for low oxygen tensions and compared with the same results obtained for atmospheric oxygen levels. In addition, the conversion of ground-state ES cells into neural precursors under low oxygen tension was also studied. Consequently, this work is expected to contribute valuable information for the improvement of current strategies for the expansion and neural differentiation of embryonic stem cells.

Results

Determination of dissolved oxygen levels in liquid culture medium

The time-dependent response of the liquid-phase oxygen levels in tissue culture plates under simulated culture conditions is shown in Figure 1. In the case of incubation under 20% O_2, the dissolved oxygen at the bottom of the culture medium layer was similar to the gas-phase tension. Under hypoxia, oxygen levels dropped swiftly, and were close to 4% within 5 h. The dissolved O_2 continued to drop at later times, and eventually reached equilibrium with the gas phase (2%). It is possible that oxygen consumption by cells at the bottom of the tissue culture plate under actual culture conditions might have accelerated the decrease of dissolved oxygen levels, thus making the actual response time much smaller. Nevertheless, cells cultured under hypoxia are exposed to higher O_2 levels for at least 5 h once every 2 days due to cell passaging.

Effect of hypoxia on mouse ES cell expansion and metabolism in the presence of LIF

To evaluate the influence of low oxygen tension (2%) on mouse ES cell expansion, cells were cultured for five consecutive passages in KO-DMEM/SR medium supplemented with LIF. Under these conditions, LIF/STAT3 signaling should contribute for self-renewal of mouse ES cells (Niwa et al., 1998). However, as can be seen in Figure 2, hypoxia resulted in a reduced cell proliferation rate. The overall cumulative fold increase (FI) in total cell number was substantially lower in 46C mouse ES cells expanded under 2% O_2 (FI = 73 ± 11) (Fig. 1a), when compared with cells maintained at atmospheric O_2 levels (FI = 6535 ± 2732) ($P < 0.05$). This resulted in a statistically significant decrease in the specific growth rate (μ) of mouse ES cells expanded at low oxygen tension (Fig. 2b). In fact, the μ value calculated for 2% O_2 was about half of the typical specific growth rate value for cells expanded in the presence of LIF (0.43 ± 0.01 day^{-1} at 2% O_2 and 0.84 ± 0.06 day^{-1} at 20% O_2). Interestingly, proliferation was partially recovered under hypoxia by supplementation of the culture medium with CHIR99021, a GSK3-specific inhibitor, in addition to LIF (μ = 0.67 ± 0.04 day^{-1} at 2% O_2 with 5 μM of the molecule, data not shown). This suggests an important role of this pathway in the regulation of stem cell functions under hypoxic conditions. Similar results were also observed for E14tg2a mouse ES cells (Fig. S1, Supplementary Data).

All proliferation results were further confirmed by cell division analysis using PKH67 fluorescent dye (da Silva et al., 2009). The determination of the number of cell divisions by flow cytometry after 2 days in culture revealed that cells expanded at low O_2 levels divided fewer times than cells cultured at 20% O_2, which reached later generations during

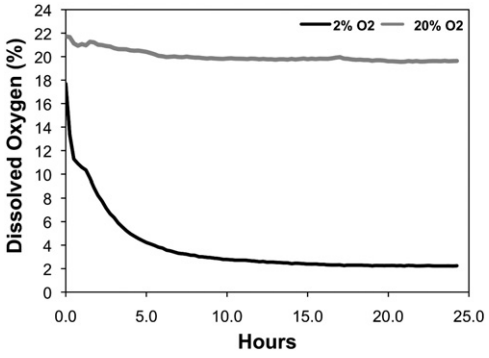

Figure 1 Dissolved oxygen in the liquid phase at the bottom of a tissue culture plate. Measurements were made in 1 mL of medium and O_2 levels were plotted as a function of time. The liquid was initially equilibrated at atmospheric oxygen levels, and the plate was then transferred to a humidified incubator either at 20 or 2% O_2 atmosphere.

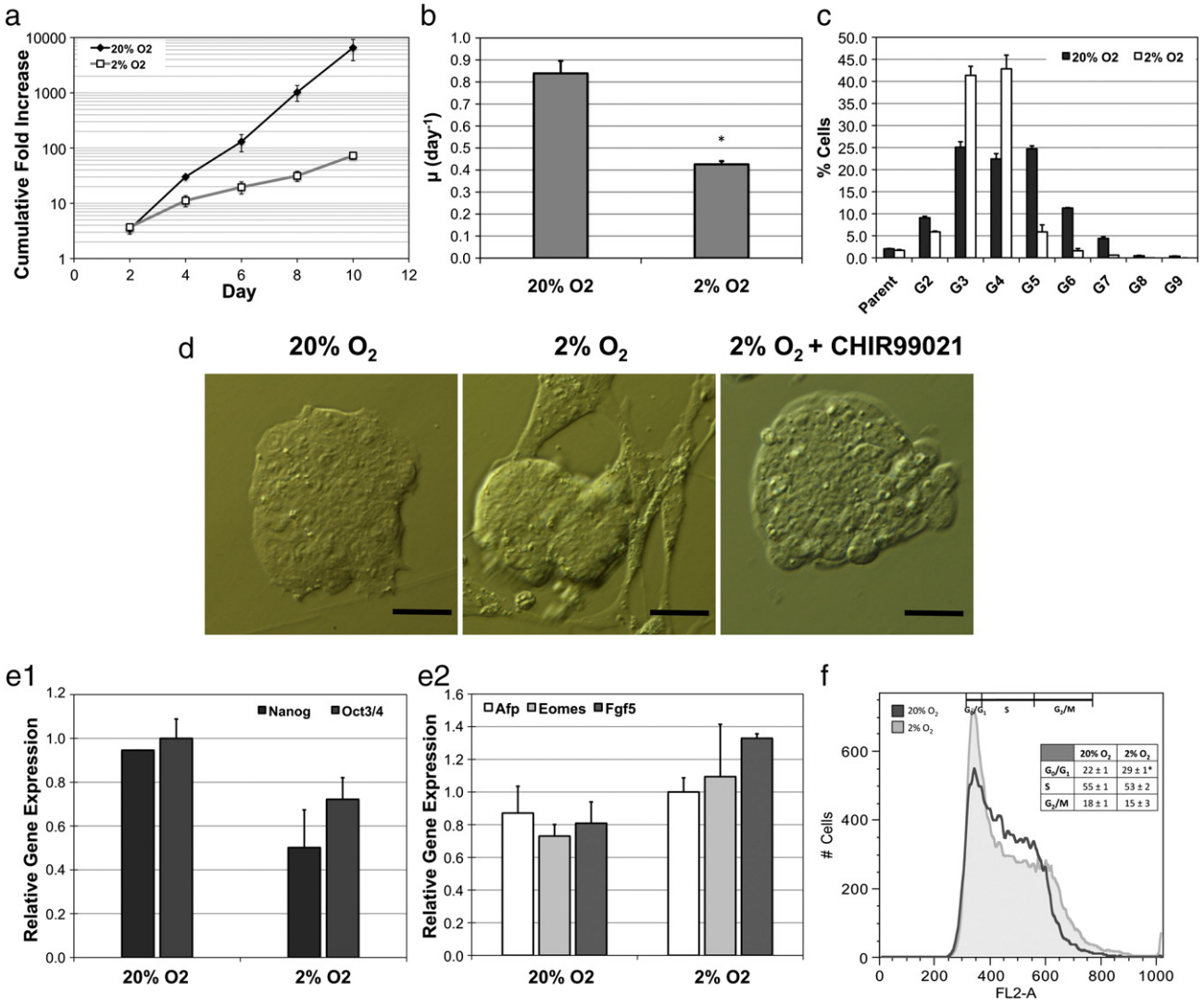

Figure 2 Hypoxia resulted in reduced mouse ES cell proliferation in the presence of LIF. **(a)** 46 C mouse ES cells were grown in KO-DMEM/SR medium supplemented with LIF. Results express the cumulative fold increase in total cell number of five consecutive passages performed in triplicate. **(b)** Specific growth rates calculated for each oxygen tension tested. Results are presented as the mean of three independent experiments. Asterisk denotes statistical significance ($P<0.05$). **(c)** Cell division analysis using PKH67 fluorescent dye. Percentage of cells in each generation (parent to G9) is shown for each oxygen tension tested. Results are presented as the mean of two independent experiments. **(d)** Mouse ES cell morphology under 20 and 2% O_2 conditions. Scale bar: 50 μm. **(e)** Real-time PCR analysis of pluripotency markers (*Nanog* and *Oct3/4*) and primed markers (*Afp*, *Eomes*, and *Fgf5*) following 46C mouse ES cell expansion in KO-DMEM/SR medium supplemented with LIF at 20 or 2% O_2 for five consecutive passages. Results are expressed as the average value of two independent experiments and are relative to gene expression at Day 0. The expression levels of the housekeeping gene *Gapdh* were used as internal control. **(f)** Cell cycle pattern analysis of mouse ES cells expanded in the presence of LIF at 2 and 20% O_2. Asterisk denotes statistical significance ($P<0.05$). All error bars represent the standard error of the mean (SEM).

the same period (Fig. 2c). Indeed, most cells (over 80%) cultured at 2% O_2 were at generations 3 and 4 after 2 days of culture (in comparison with 47% for 20% O_2), whereas a significant fraction of cells (over 35%) at 20% O_2 had already reached generations 5 and 6. Furthermore, low oxygen tension resulted in a decrease in cell viability throughout time in culture. In fact, after five consecutive passages, cell viability (assessed by trypan blue exclusion test) at 2% O_2 was 77 ± 2%, and at 20% O_2 it was 91 ± 2% ($P<0.05$). Together with a decrease in the number of cell divisions, this result helps in explaining the reduced overall cell fold increase and the lower specific growth rates obtained at low oxygen levels. Analysis of cell morphology also revealed striking differences between cells expanded at 2% O_2 and cells maintained at atmospheric O_2 levels (Fig. 2d). Under normoxia (20% O_2), in the presence of LIF, cells displayed typical compact colony morphology, a characteristic of undifferentiated ES cells. On the other hand, when cultured under hypoxia (2% O_2), cells became largely flattened and sharpen at the edges of the colonies, a fibroblast-like morphology typical of early commitment. Nevertheless, addition of 5 μM of GSK3-specific inhibitor CHIR99021 was able to recover typical

compact ES cell morphology in hypoxia (Fig. 2d), which provides additional evidence of the positive effect of GSK3 inhibition at low oxygen tensions (Mottet et al., 2003). Quantification of pluripotency markers (Oct-4 and Nanog) by flow cytometry did not reveal any statistically significant differences in the levels of these proteins, as measured by the peak mean intensity values (data not shown), with more than 95% Oct-4- and Nanog-positive cells under both conditions tested (Fig. S2, Supplementary Data).

The results so far indicate that expansion of mouse ES cells in the presence of LIF at low oxygen tensions can result in a reduction of the proliferation rate, increase in cell death, and morphology changes, although pluripotency markers remained expressed in a high percentage of cells. To further confirm that under these conditions hypoxia leads to an early priming of mouse ES cells toward commitment, quantitative real-time polymerase chain reaction (RT-PCR) was performed after cell expansion (Fig. 2e). It is possible to observe a tendency for reduction in the relative expression of pluripotency markers (*Oct3/4* and *Nanog*) under hypoxia. At the same time, there was a slight increase in the expression of primed markers (*Afp*, *Eomes*, and *Fgf5*) at 2% O_2, which is more evident for the primitive ectoderm marker *Fgf5*. In addition, the cell cycle profile was also assayed by flow cytometry for cells expanded at 2 and 20% O_2 (Fig. 2f). Mouse ES cells cultured under normoxia (20% O_2) showed a typical cell cycle profile, displaying a large proportion of cells in the S phase, resulting from the absence of G_1 checkpoints (Burdon et al., 2002). However, when maintained at low oxygen levels, the proportion of cells in G_0/G_1 increases significantly ($P<0.05$), which may denote a modification in the G_1-phase arrest that is characteristic of early differentiation (Burdon et al., 2002). Therefore, our results suggest that hypoxia induces an early priming of mouse ES cells toward differentiation when LIF is used for maintenance of the pluripotent state.

In addition to affecting mouse ES cell proliferation and pluripotency, low oxygen levels also influenced cell metabolism (Fig. 3). The average consumption/production rates (in mM/day) of glucose, glutamine, lactate, and ammonia were not substantially affected by the reduction in oxygen level, remaining fairly constant for cells expanded at 2% O_2 and 20% O_2 (Fig. 3a). More importantly, concentrations of potentially toxic metabolites (lactate and ammonia) did not reach levels considered to be inhibitory for mammalian cells (Ozturk et al., 1992). However, since hypoxia resulted in lower cell numbers, a better comparison of both conditions should be made using the specific (per cell) consumption/production rates. This revealed a significantly higher ($P<0.05$) production of lactate per cell under hypoxia (20.3 ± 1.1 pmol/(cell.day) versus 11.7 ± 2.1 pmol/(cell.day) at 20% O_2), which might be expected under low oxygen tensions as the result of increased anaerobic metabolism. In addition, a tendency for slightly higher consumption of glutamine per cell was observed at low oxygen levels (1.2 ± 0.1 pmol/(cell.day) at 2% O_2 and 0.8 ± 0.1 pmol/(cell.day) at 20% O_2, $P=0.056$).

Evidence of these metabolic changes under hypoxic conditions can also be seen when analyzing the apparent metabolic yields of the culture (Figs. 3b and c). Even though the apparent lactate from glucose yield ($Y'_{lactate/glucose}$) was

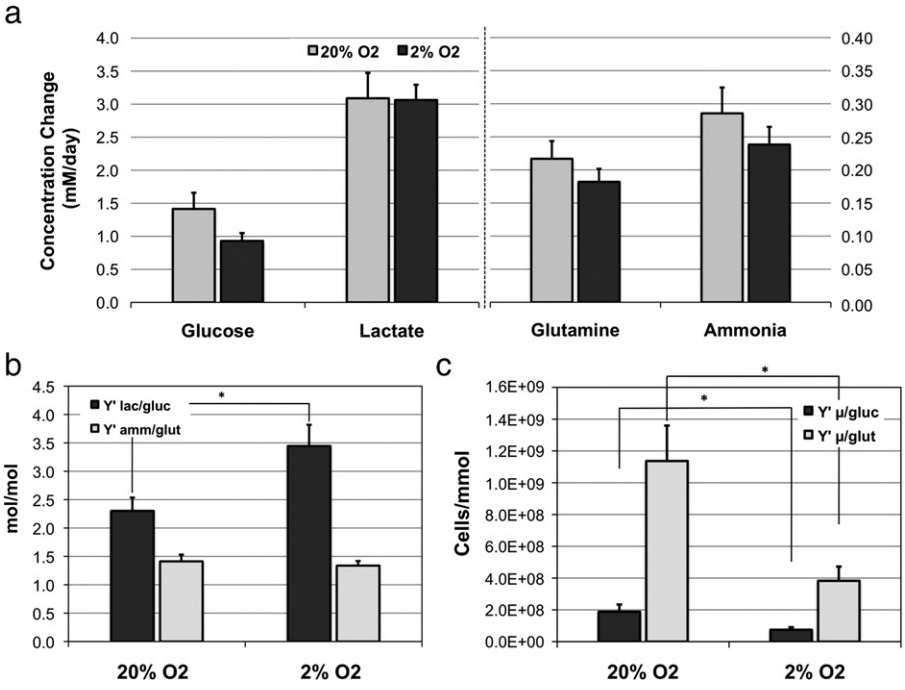

Figure 3 Influence of hypoxia on mouse ES cell metabolism during expansion with LIF. (a) Average concentration change in glucose, lactate, glutamine, and ammonia. (b) Apparent yields of lactate from glucose ($Y'_{lactate/glucose}$) and ammonia from glutamine ($Y'_{ammonia/glutamine}$) calculated for 2 and 20% O_2 conditions. (c) Cell yields from glucose ($Y'_{\mu/glucose}$) and glutamine ($Y'_{\mu/glutamine}$) calculated for low oxygen levels and for normal (20%) oxygen levels. Cells were expanded in KO-DMEM/SR medium supplemented with LIF and results express the average values of five consecutive passages performed in triplicate. Asterisks denote statistical significance ($P<0.05$).

above 2 mol of lactate per mol of glucose (the theoretical limit) for both oxygen tensions tested, $Y'_{lactate/glucose}$ at 2% O_2 was substantially higher than at 20% O_2 (Fig. 3b) ($P<0.05$). Production of lactate from other sources, like glutamine, explains why yields greater than 2 can be obtained (Reitzer et al., 1979). However, according to our results, the relevance of alternative metabolic pathways, such as glutaminolysis, seems to be greater under hypoxia. Interestingly, no differences were seen in the values of the apparent ammonia from glutamine yield ($Y'_{ammonia/glutamine}$) (Fig. 3b), but cell yields from glucose and glutamine calculated for low oxygen levels were significantly lower than the ones obtained for atmospheric (20%) oxygen level (Fig. 3c, $P<0.05$), indicating that mouse ES cell metabolism under expansion conditions in the presence of LIF is less efficient under hypoxia.

Effect of hypoxia on expansion and metabolism of ground-state pluripotent mouse ES cells

The results presented in the previous section are relative to ES cells expanded under conditions that activate LIF/STAT3 signaling in order to maintain cell pluripotency. However, as previously reported, hypoxia suppresses LIF/STAT3 signaling via hypoxia-inducible transcription factor 1-alpha (HIF-1α) (Jeong et al., 2007), which may explain the apparent early differentiation induced by low levels of O_2. Nevertheless, maintenance of ground-state pluripotency can be attained in culture by inhibition of FGF4/ERK and GSK3 signaling, a mechanism that is independent and upstream of LIF/STAT3 (Ying et al., 2008). Thus, the influence of low oxygen tensions on ground-state ES cell proliferation and metabolic profile may result in different outcomes.

To study this possibility, mouse ES cells were cultured for five consecutive passages in *i*STEM serum-free medium to sustain ground-state pluripotency, either under atmospheric oxygen tension (20% O_2) or reduced oxygen levels (2% O_2). The proliferation of mouse ES cells under these conditions was not affected and the overall cumulative fold increase in total cell number was similar (FI = 3911 ± 1429 for 20% O_2 and FI = 2646 ± 488 for 2% O_2), independently of the oxygen level used (Fig. 4a). This resulted in identical growth rate values for both conditions tested (0.82 ± 0.04 day^{-1} for 20% O_2 and 0.79 ± 0.02 day^{-1} for 2% O_2). Similar results were also observed for E14tg2a mouse ES cells (Fig. S3, Supplementary Data). Interestingly, cell viability at 2% O_2 was always significantly lower ($P<0.05$ for all data points) when compared with cell viability at 20% O_2 throughout time in culture (Fig. 4b), indicating a detrimental effect of hypoxia on cell viability that was already seen for mouse ES cells expanded in the presence of LIF. In addition, over 95% of cells were positive for Oct-4 and Nanog, either at low or at atmospheric oxygen tensions, as quantified by flow cytometry (Fig. S4, Supplementary Data).

Mouse ES cell expansion at clonal densities was also performed as a rigorous test to further evaluate the effectiveness of low oxygen levels in sustaining ground-state ES cells (Fig. 4c). Cells were seeded at low densities and maintained in *i*STEM serum-free medium for 6 days with medium change at Days 2 and 4. After single-cell deposition, both oxygen tensions gave rise to ES cell colonies with a similar efficiency (23 ± 5 and 23 ± 2% for low and atmospheric oxygen levels, respectively). However, colony size distribution was more homogeneous at 20% O_2 (Fig. 4d), and the average colony diameter was smaller (72 ± 11 μm) when compared to 2% O_2 (99 ± 21 μm). Thus, this result indicates that at clonal densities, cells cultured in a reduced oxygen atmosphere give rise to larger colonies. In addition, cell division analysis using PKH67 fluorescent dye by flow cytometry revealed that cells expanded at low O_2 levels divided more times under these conditions, reaching higher percentages of cells in later generations when compared with 20% O_2 (Fig. 4e). Moreover, mouse ES cells expanded in a reduced oxygen atmosphere displayed a cell cycle profile identical to cells cultured under normoxia. Both populations showed a profile characteristic of ES cells, with a large proportion of cells in the S phase (52 ± 2 and 53 ± 2% of cells at reduced O_2 levels and normoxia, respectively), resulting from the absence of G_1 checkpoint. No statistically significant differences were observed between the cell percentages in G_0/G_1 for the O_2 levels tested (28 ± 1% of cells at 2% O_2 and 26 ± 1% of cells at 20% O_2). Real-time PCR analysis also shows no major differences in the expression levels of pluripotency markers (*Oct3/4* and *Nanog*) between cells maintained under different oxygen conditions. In addition, hypoxia did not result in increased expression of primed markers, such as *Fgf5*, *Afp*, or *Eomes* (Fig. S5, Supplementary Data). These results highlight that oxygen levels did not affect the ground-state pluripotency of authentic ES cells. Nevertheless, despite possessing a negative influence on cell viability under ground-state culture conditions, hypoxia also appeared to accelerate cell proliferation, which was confirmed by flow cytometry using the PKH67 fluorescent dye. Therefore, the overall proliferation rate was not affected and similar cell numbers were produced in both oxygen tensions tested.

The effect of low oxygen levels on the metabolism of ground-state mouse ES cells was also evaluated (Fig. 5). The average consumption/production rates (in mM/day) of glucose, glutamine, lactate, and ammonia were calculated for 2% O_2 and 20% O_2 conditions (Fig. 5a). The reduction in oxygen tension did not affect glutamine consumption and ammonia production. Nonetheless, hypoxia seemed to increase to some extent glucose consumption and lactate production. Analysis of the specific (per cell) consumption/production rates also supports this evidence, and under hypoxia an increase in glucose consumption (10.2 ± 1.7 pmol/(cell.day) versus 4.1 ± 0.4 pmol/(cell.day) at 20% O_2) ($P<0.05$) was also accompanied with an increase in lactate production (14.8 ± 2.2 pmol/(cell.day) versus 9.3 ± 1.3 pmol/(cell.day) at 20% O_2), which might be expected under low oxygen tensions as the result of an increased anaerobic metabolism. Importantly, concentrations of potentially toxic metabolites, especially lactate, did not reach inhibitory levels. The apparent metabolic yields were also calculated for the expansion of ground-state ES cells at low oxygen levels (Figs. 5b and c). Interestingly, in contrast with the results obtained for mouse ES cell expansion with LIF, no significant differences were seen in the values of the apparent lactate from glucose yield ($Y'_{lactate/glucose}$) and the apparent ammonia from glutamine yield ($Y'_{ammonia/glutamine}$) (Fig. 5b). Cell yields from glucose and glutamine calculated for 2 and 20% O_2 were comparable and within the error, indicating that mouse ES cell metabolism during

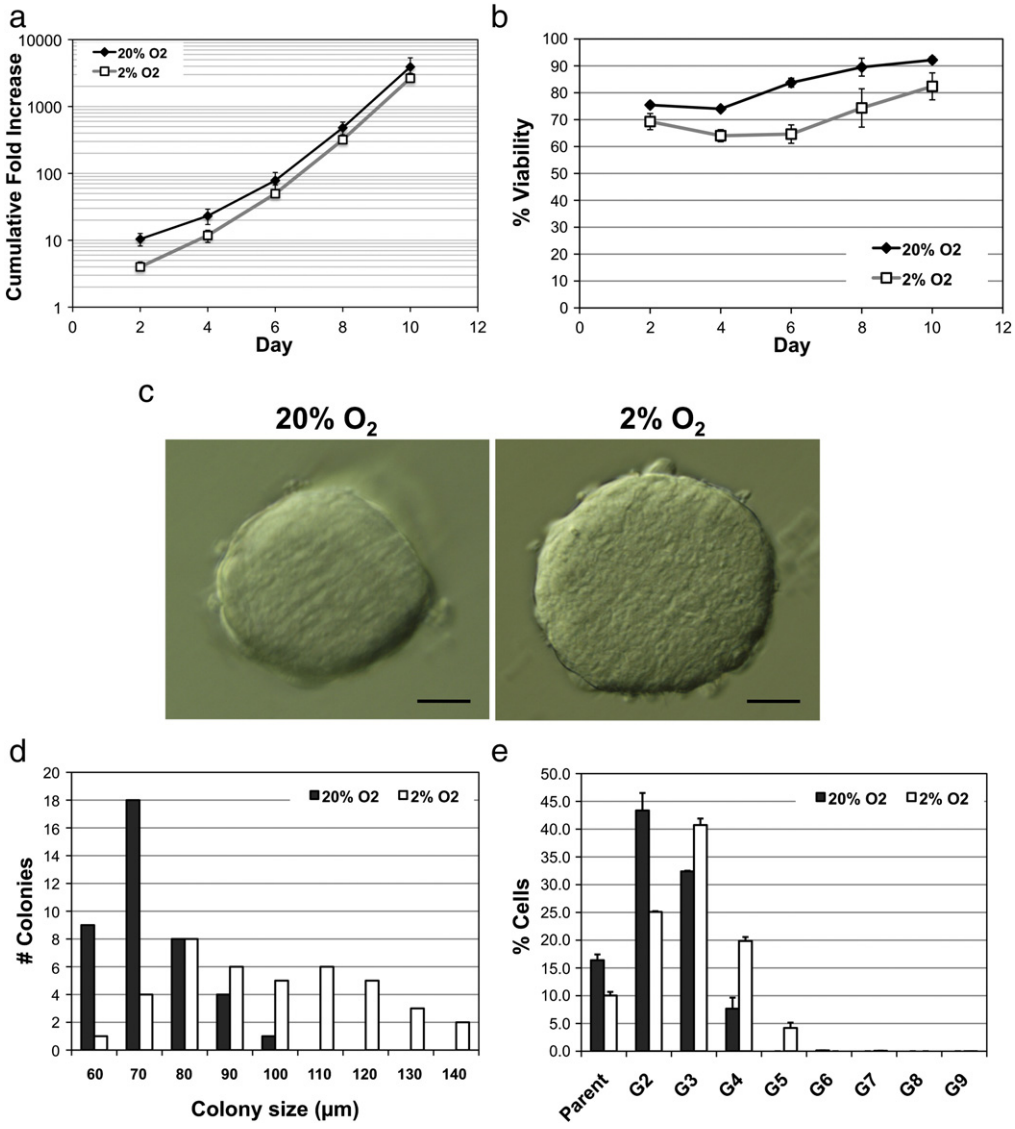

Figure 4 Influence of low oxygen levels on ground-state mouse ES cell expansion. **(a)** Influence of oxygen tension on 46C mouse ES cell cumulative fold increase during expansion in *i*STEM serum-free medium. Results express the cumulative fold increase in total cell number of five consecutive passages performed in triplicate. **(b)** Percentage of cell viability for each oxygen tension tested. Results are presented as the mean of three independent experiments. **(c)** Mouse ES cell colonies at 20 and 2% O_2 conditions. Scale bar: 50 µm. **(d)** Colony diameter (in µm) distribution for 20 and 2% O_2 conditions. A total of 40 colonies were measured from four independent experiments. **(e)** Cell division analysis using PKH67 fluorescent dye. Percentage of cells in each generation (parent to G9) is shown for each oxygen tension tested. Results are presented as the mean of two independent experiments. All error bars represent the standard error of the mean (SEM).

expansion under ground-state conditions was not negatively influenced by a hypoxic environment.

Neural commitment of ground-state mouse ES cells under hypoxic conditions

We next reasoned that oxygen tension control during neural commitment of ground-state ES cells could potentially be used for improved efficiency in the generation of ES cell-derived neural progenitors. Therefore, ground-state ES cells (expanded in *i*STEM serum-free medium) were collected and plated onto gelatin-coated tissue culture plates and incubated for 8 days in neural differentiation medium. Under these conditions, elimination of inductive signals for alternative fates conducts ES cells to develop into neural precursors through autocrine FGF signaling (Ying et al., 2003b).

The neural commitment protocol was carried out under either atmospheric oxygen tension (20% O_2) or reduced oxygen levels (2% O_2). Plating efficiency was similar for both oxygen tensions studied, and total cell numbers obtained throughout time in culture did not differ considerably until Day 5 (Fig. 6a). However, starting at Day 6, 20% O_2 conditions promoted significantly higher fold increase values in total cell number, reaching a value of 51 ±7 at Day 8, while for 2% O_2 conditions the final fold

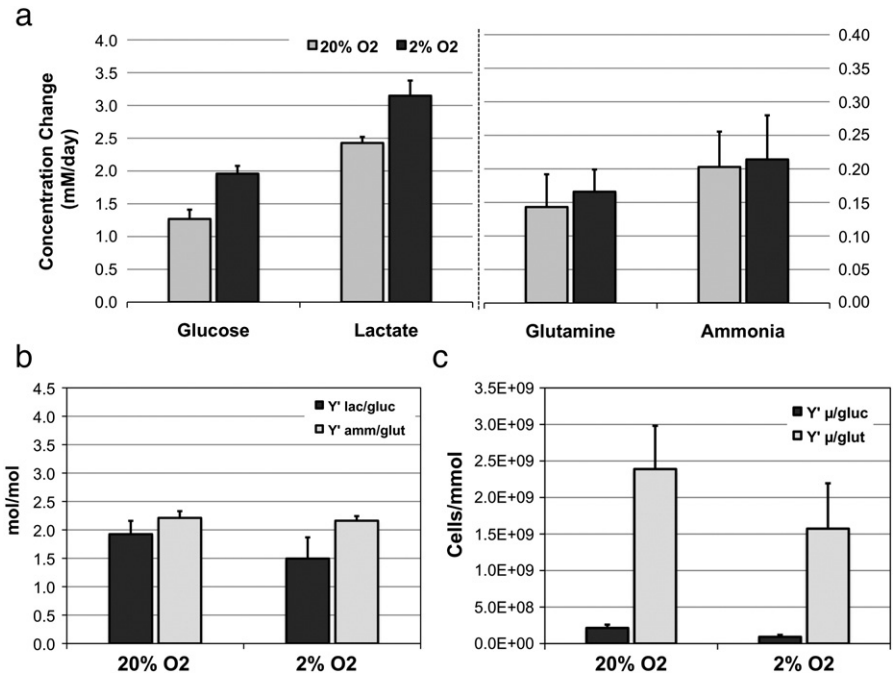

Figure 5 Influence of hypoxia on the metabolism of ground-state mouse ES cell expansion. **(a)** Average concentration change in glucose, lactate, glutamine, and ammonia levels. **(b)** Apparent yields of lactate from glucose ($Y'_{lactate/glucose}$) and ammonia from glutamine ($Y'_{ammonia/glutamine}$) calculated under 2 and 20% O_2 conditions. **(c)** Cell yields from glucose ($Y'_{\mu/glucose}$) and glutamine ($Y'_{\mu/glutamine}$) calculated for low oxygen levels and for atmospheric (20%) oxygen levels. Cells were expanded in *i*STEM serum-free medium and results express the mean values of five consecutive passages performed in triplicate.

increase was about half of this value (22 ± 2). During the same period (from Day 6 to Day 8) cell viability at 2% O_2 was substantially reduced (around 47% viability at Day 8), explaining the differences observed in cell fold increase values (Fig. 6b).

The use of a green fluorescent protein (GFP) knock-in reporter ES cell line (46C) allowed the examination of the process by which ES cells acquire neural identity since the open-reading frame of the Sox1 gene was replaced with the coding sequence of GFP. Sox1 is an early marker of neuroectoderm in the mouse embryo and can be used to study neural differentiation *in vitro* (Ying et al., 2003b). Thus, evaluation of neural commitment kinetics is possible by flow cytometry analysis (Fig. 6c). This revealed that the maximum expression of Sox1-GFP was reached faster at 2% O_2 than at 20% O_2, and by Day 4 cells maintained under low oxygen levels were already over 80% Sox1 positive (83.8 ± 3.1%) whereas under 20% O_2 the percentage of Sox1-positive cells was only 65.6 ± 7.3%. Nevertheless, the maximum level of Sox1-GFP cells was identical for both oxygen tensions tested (85.9 ± 1.5% at 2% O_2 and 83.0 ± 1.9% at 20% O_2, both at Day 5). Interestingly, at atmospheric oxygen tension the percentage of Sox1-positive cells remained fairly constant after reaching the maximum at Day 5. However, a decrease in Sox1 levels occurred for low oxygen tension, and by Day 8 it was significantly lower than at 20% O_2, possibly indicating a further differentiation into more mature neural cells. In fact, by Day 8, flow cytometry quantification of neuronal class III β-tubulin (Tuj1) revealed a slightly higher percentage of neuronal cells at low oxygen tension (Fig. 6d).

Sox1-positive neural progenitors are nevertheless a transient population. Hence, to evaluate the influence of low oxygen tension on further neuronal differentiation, cells maintained at 20% O_2 were collected at Day 6 of neural commitment and replated onto tissue culture plates pre-coated with polyornithine and laminin, as described previously (Pollard et al., 2006). At both oxygen tensions tested, cells readily adhered to the surface and showed typical morphology, as indicated by the establishment of complex branches and cell-to-cell contacts (Fig. 6e). However, no significant differences in terms of neuronal maturation dynamics were seen when comparing 2% O_2 and 20% O_2 (Fig. 6f), indicating that oxygen tension did not affect this process at least under these culture conditions. However, our results appear to indicate a beneficial effect of hypoxia on early commitment of ground-state ES cells toward primitive neuroectoderm.

In parallel, the metabolism of neural commitment of ground-state mouse ES cells was also evaluated (Fig. 7). During neural commitment of ground-state mouse ES cells variations in the consumption/production rates of important metabolites were observed. In general, for both oxygen tensions tested, the specific (per cell) consumption/production rates decreased throughout time in culture (Fig. 7a), consistent with higher initial cell growth followed by adaptation of the cells to the culture environment. Interestingly, very high levels of glucose consumption were observed, especially during the first days in culture (until Day 2). In fact, the medium used (RHB-A) displays glucose levels (35 mM) that are substantially higher than what is typically used in other culture media (e.g., 20 mM), while at the same time

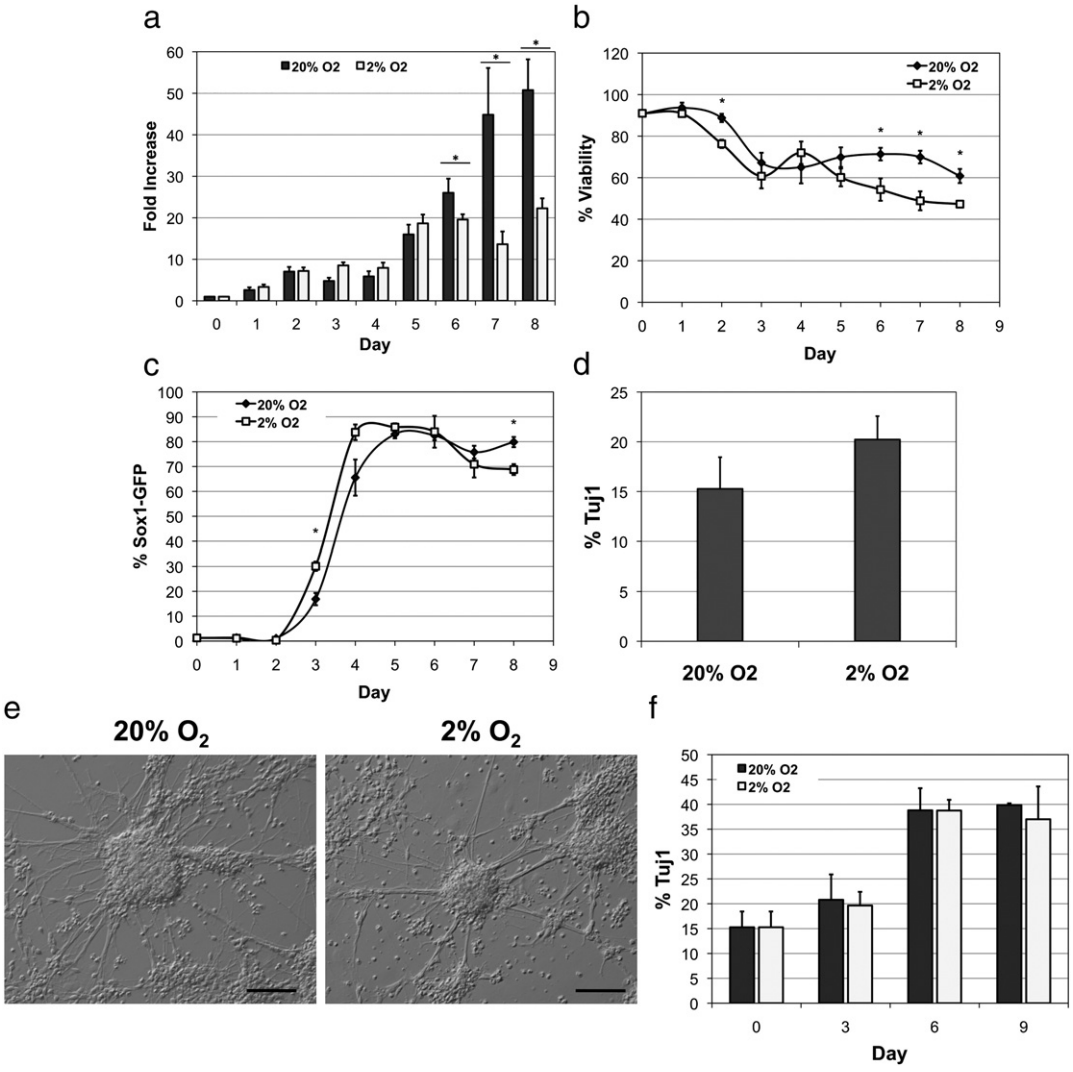

Figure 6 Influence of low oxygen levels on neural commitment of ground-state mouse ES cells. **(a)** Effect of oxygen tension on total cell numbers. Cells were grown in RHB-A serum-free medium. Results express the fold increase in total cell number at each day of neural commitment. **(b)** Percentage of cell viability for each oxygen tension tested throughout time in culture. **(c)** Percentage of Sox1-GFP-positive cells during neural commitment at different O_2 levels. **(d)** Flow cytometry quantification of neuronal class III β-tubulin (Tuj1)-positive cells at Day 8 of neural commitment. **(e)** Cell morphology after replating of Sox1-positive neural progenitors and culture for 6 days in RHB-A serum-free medium. Scale bar: 100 μm. **(f)** Percentage of Tuj1-positive cells during neuronal differentiation of neural progenitors. All results are presented as the mean of three independent experiments performed in duplicate. Error bars represent the standard error of the mean (SEM). Asterisks denote statistical significance ($P<0.05$).

glutamine concentrations are lower (0.07 mM as compared to 2 mM in typical mammalian cell culture media). This also resulted in high lactate-specific production rates until Day 4 of neural commitment. However, no differences between the results obtained for both oxygen tensions were seen during this period. Nevertheless, starting at Day 4, hypoxia led to substantially higher lactate production rates. Moreover, glucose-specific consumption rates were also significantly higher by Day 8 at low oxygen levels. This result might be due to an increase in anaerobic metabolism at low oxygen tensions. Importantly, between Day 4 and Day 6, lactate concentrations were higher than 20 mM, a value known to be inhibitory for other stem cells (e.g., mesenchymal) under hypoxia (Schop et al., 2009). This may have affected cell viability, possibly explaining, at least in part, the limited cell growth and increased cell death observed under these conditions when compared to normoxia (Figs. 6a and b).

The apparent yields of lactate from glucose ($Y'_{lactate/glucose}$) during neural commitment were also calculated (Fig. 7b). Interestingly, no differences were seen between the two oxygen levels tested. Furthermore, $Y'_{lactate/glucose}$ values were always below 2 mol of lactate per mol of glucose (the theoretical limit) for both oxygen tensions tested, suggesting that alternative metabolic pathways, such as glutaminolysis, were not so relevant under these conditions. In fact, during the first 2 days of commitment, $Y'_{lactate/glucose}$ values were significantly lower when compared with later times in culture. After this period, $Y'_{lactate/glucose}$ values increased and remained fairly constant until Day 8. The low glutamine concentrations in the culture medium used may explain these results,

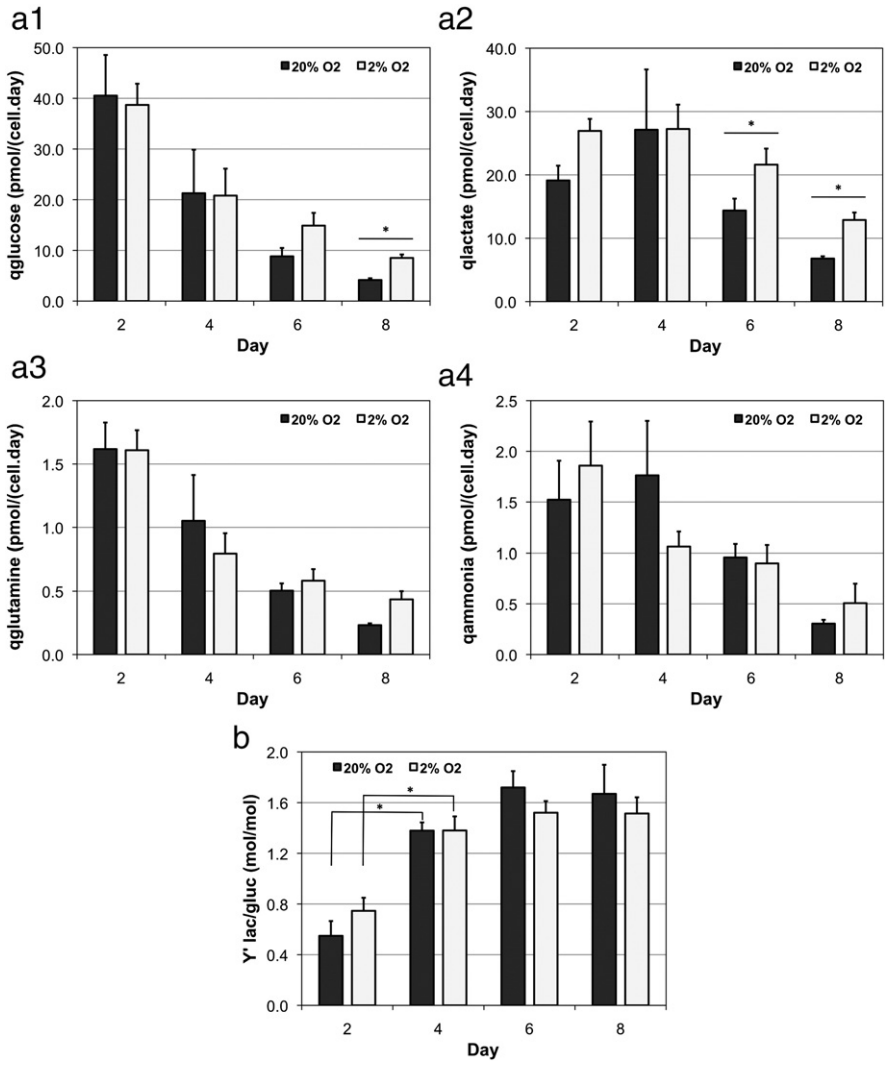

Figure 7 Metabolism of ground-state mouse ES cells during neural commitment at different oxygen levels. **(a)** Specific consumption/production rates of glucose, lactate, glutamine, and ammonia under 2 and 20% O_2 conditions during neural commitment. **(b)** Apparent yield of lactate from glucose ($Y'_{lactate/glucose}$) calculated under 2 and 20% O_2 conditions during neural commitment. Cells were cultured in RHB-A serum-free medium and results express the mean of three independent experiments performed in duplicate. Error bars represent the standard error of the mean (SEM). Asterisks denote statistical significance ($P<0.05$).

underscoring the importance of this amino acid for biosynthetic pathways, namely protein synthesis, which is more evident during the first days in culture.

Discussion

In most mammalian tissues, cells are exposed to oxygen tensions that are substantially lower than atmospheric levels (Ivanovic, 2009). Hypoxia, or physiological oxygen tension, is expected to impact not only cell growth and phenotype but also cellular energetics and metabolism. Thus, in order to evaluate how oxygen levels influence the proliferation and neural differentiation of ground-state embryonic stem cells, we performed a comprehensive analysis of proliferation kinetics, cell viability, protein and gene expression, cell cycle, and metabolic profiles under different oxygen tensions.

When cells were expanded under serum-free conditions with LIF, growth of mouse ES cells was significantly reduced at 2% O_2 conditions. However, the fraction of cells expressing Oct-4 and Nanog, as assessed by flow cytometry, was not affected, despite morphological changes indicative of some early differentiation. In addition, quantitative real-time PCR and cell cycle profile analysis further indicated evidence of early priming of cells toward differentiation. These results suggest that hypoxic conditions prompt mouse ES cells early commitment when LIF is used to maintain cell pluripotency. In fact, LIF/STAT3 signaling is suppressed by HIF-1α, which results in hypoxia-induced *in vitro* differentiation (Jeong et al., 2007). Our findings are consistent with previous studies that also reported similar effects of hypoxia on mouse ES cell expansion (Powers et al., 2008). Nevertheless,

despite the effects of hypoxia on stem cell function (Covello et al., 2006), the blockage of GSK3 signaling by addition of CHIR99021 to the culture medium had a positive effect in cells maintained at low oxygen levels with LIF. Inhibition of GSK3 signaling resulted in partial recovery of specific growth rate values and typical compact mouse ES cell morphology. This may indicate a pivotal role of this pathway in the regulation of cell functions under hypoxic conditions (Mottet et al., 2003). Moreover, specific pharmacological inhibition of GSK3 has been shown to maintain undifferentiated ES cells through activation of the canonical Wnt pathway (Sato et al., 2004). Consequently, single blockade of GSK3 restrains neural differentiation, while enhancing growth capacity (Ying et al., 2008). This mechanism might have contributed to the partial recovery of ES cell phenotype under hypoxic conditions with LIF and CHIR99021 supplementation.

Cell metabolism was also altered under hypoxic conditions in the presence of LIF. Higher lactate production rates, indicative of an increased anaerobic metabolism, were obtained for low oxygen tensions. This effect has also been reported for other stem cell populations (e.g., mesenchymal), simultaneously with an increase in glucose consumption (Follmar et al., 2006). Additionally, production of lactate from other sources, especially glutamine, was also more relevant in hypoxia, as indicated by the increase in the apparent lactate from glucose yield to values well above 2. According to our results, it appears that a less efficient cell metabolism arises during expansion of mouse ES cells in the presence of LIF under hypoxic conditions compared to normoxia.

However, the effect of hypoxia in ground-state mouse ES cells was somewhat different. Self-renewal of authentic, ground-state ES cells in culture does not depend on LIF/STA3 signaling. It is rather due to inhibition of FGF4/ERK and GSK3 signaling (Ying et al., 2008), a mechanism that is independent and upstream of LIF/STAT3. Under these conditions, hypoxia did not affect cell proliferation, which actually appeared to be increased, especially at clonal densities. Nevertheless, low oxygen levels had a negative impact on cell viability. No signs of differentiation were observed, as assessed by the analysis of pluripotency markers, cell morphology, and cell cycle profile. Thus, high numbers of ground-state ES cells could be generated under hypoxic conditions, despite the negative influence on cell viability. The contribution of GSK3 inhibition under ground-state conditions appears to extend beyond limiting differentiation. It is known that this pathway modulates metabolic activity, biosynthetic capacity, and overall viability (Doble and Woodgett, 2003). Nevertheless, our results show that GSK3 inhibition does not restore cell viability under hypoxia. Alternatively, reduced GSK3 activity may exert a global modulation of cell metabolism and biosynthetic capacity rather than having a direct antiapoptotic action, since antiapoptotic factors were not found under ground-state conditions (Ying et al., 2008). In theory, this could be overcome if the negative influence of hypoxia-related cell death could be minimized by the use of chemical inhibitors to generate higher numbers of pluripotent ES cells (Duval et al., 2004; Krishnamoorthy et al., 2009; Watanabe et al., 2007).

Under ground-state culture conditions, hypoxia seemed to increase to some extent glucose and lactate metabolism, similar to that obtained for mouse ES cell expansion in the presence of LIF, and to that reported for adult stem cells (Follmar et al., 2006). Nevertheless, no differences were observed in the values of the metabolic yields, indicating that mouse ES cell metabolism during expansion under ground-state conditions is not negatively influenced by a hypoxic environment. Overall, our findings indicate that ground-state ES cells can be maintained under hypoxic conditions and generate comparable numbers of cells without differentiation, while maintaining an efficient cell metabolism.

We next focused on evaluating how hypoxia influences the neural commitment of ground-state mouse ES cells. Differentiation of ES cells toward the neural lineage is characterized by progression through different stages resembling neurogenesis (Sutter and Krause, 2008). When signals for alternative fates are eliminated, mouse ES cells readily develop into neuroectodermal precursors in adherent monolayer, due to autocrine FGF signaling (Ying et al., 2003b). Since the embryo is subjected to a hypoxic environment (Rodesch et al., 1992), we reasoned that low oxygen tensions would impact the neural commitment of ground-state mouse ES cells.

Hypoxia had a negative effect on cell viability after 6 days of neural commitment. In fact, potentially inhibitory levels of lactate were reached in the culture medium during this period, which may explain this outcome. Nevertheless, Sox1-positive neural progenitors were generated faster at 2% O_2, although similar maximum levels of Sox1-positive cells were obtained in both oxygen tensions tested. Furthermore, after reaching the maximum by Day 5, a decrease in Sox1 levels occurred for low oxygen tension, and by Day 8 it was significantly lower than at 20% O_2. This was accompanied by a slight increase in the percentage Tuj1-positive cells, indicating a further differentiation in more mature neural cells. Despite this, oxygen tension did not affect neuronal maturation after replating of neural progenitors on laminin-coated surfaces. Thus, hypoxia only appears to have a positive effect on the early commitment of ground-state ES cells toward primitive neuroectoderm.

Cell metabolism during neural commitment was also influenced by hypoxic conditions. High levels of glucose consumption and lactate production were seen for 2 and 20% O_2 during the first days of commitment. Nevertheless, later in culture, hypoxia led to substantially higher glucose and lactate consumption/production rates due to an increase in anaerobic metabolism at low oxygen tensions. Interestingly, very low yields of lactate from glucose were obtained during the first 2 days of commitment. Also, despite increasing significantly at later days, $Y'_{lactate/glucose}$ values were always below 2 mol of lactate per mol of glucose (the theoretic limit) for both oxygen tensions tested, indicating that alternative metabolic pathways to glycolysis, such as glutaminolysis, were not favored under these conditions. In fact, glutamine concentrations in the culture medium used are within the range of limiting levels described for mammalian cell culture (0.5 to 2 mM (Vriezen et al., 1997)), and under these circumstances cells may only use glutamine for biosynthesis during neural commitment.

Conclusions

This work revealed that hypoxia, or reduced oxygen tension, can differently impact mouse ES cells depending on the specific signaling pathway that is being used for maintenance

of cell pluripotency. When LIF/STAT3 signaling was responsible for maintaining ES cells self-renewing, hypoxia had a negative effect on cell proliferation and viability. Furthermore, it exerted a proactive effect on differentiation, and cells showed signs of early commitment. On the contrary, low oxygen levels did not influence the final cell numbers of mouse ES cells cultured under ground-state conditions. These cells are maintained in culture by inhibition of FGF4/ERK and GSK3 signaling and, despite affecting cell viability, hypoxia did not induce cell differentiation. Nevertheless, during neural commitment, low oxygen tension exerted a positive effect on early differentiation of ground-state ES cells. Thus, it is possible to conclude that, depending on the specific signaling pathways explored, oxygen levels may be a potentially important parameter to consider during the development of strategies for ES cell expansion and controlled differentiation.

Materials and methods

Cell Lines

In the present studies, the E14tg2a and 46C mouse ES cell lines were used as model systems. The 46C cell line (established at the laboratory of Professor Austin Smith, Wellcome Trust Centre for Stem Cell Research, University of Cambridge, England, UK) contains a green fluorescent protein (GFP) knock-in at the Sox1 locus (neuroepithelial marker gene) and can be induced to undergo neural commitment under serum-free conditions (Diogo et al., 2008; Ying et al., 2003b). E14tg2a and 46C mouse ES cells were kept cryopreserved in liquid nitrogen until further use.

Determination of dissolved oxygen levels in liquid medium

To examine the response of dissolved oxygen levels in the liquid medium under simulated culture conditions, a 24-channel SDR SensorDish Reader (PreSens) for on-line monitoring was used to measure O_2 tension at the bottom of a liquid layer in multiwell culture plates with integrated optical-chemical oxygen sensors. The liquid was initially equilibrated at atmospheric oxygen levels, and the plate was then transferred to a humidified incubator either at 20 or 2% O_2 gas phase. The dissolved O_2 levels were measured as a function of time.

Expansion of mouse ES cells

On thawing, mouse ES cells were expanded on gelatinized tissue culture plates (0.1% (v/v) gelatin in phosphate-buffered saline (PBS; Gibco), diluted from a 2% stock solution; Sigma) using Knockout Dulbecco's modified Eagle's medium (DMEM; Gibco) supplemented with 15% (v/v) Knockout serum-replacement (SR; according to the manufacturer's instructions, Gibco), 2 mM glutamine (Gibco), 1% (v/v) penicillin (50 U/mL)/streptomycin (50 μg/mL) (Pen/Strep; Gibco), 1% (v/v) nonessential amino acids (Sigma), and 1 mM β-mercaptoethanol (β-ME; Sigma); Knockout serum-free medium (KO-DMEM/SR) was supplemented with 0.1% (v/v) LIF (human LIF produced in house by HEK-293 cells). In selected experiments, the GSK3-specific inhibitor CHIR99021 (Stemgent) was also added to the culture medium at a final concentration of 5 μM. Alternatively, the cells were expanded in *i*STEM serum-free medium (Stem Cell Sciences Inc.) for culture of authentic, ground-state mouse ES cells. This culture medium is supplemented with three chemical inhibitors that eliminate differentiation signals, sustaining mouse ES cell self-renewal and maintaining the pure ES cell ground state, as previously described (Ying et al., 2008).

The cells were cultured either under atmospheric oxygen tension (20% O_2) or reduced oxygen atmosphere (hypoxic chamber connected to a Proox Model 21 controller set up at 2% O_2; BioSpherix) at 37 °C in a 5% CO_2 humidified incubator. Cells were dissociated every 2 days using Accutase solution (Sigma) and replated at the same initial cell density (20 000 cells/cm^2). At each passage, viable and dead cell numbers were determined by counting in a hemocytometer under an optical microscope using the trypan blue dye exclusion test (Gibco). Assuming exponential growth, the apparent specific growth rate, μ (day^{-1}), was calculated as $\mu = \ln(X_f/X_i)/\Delta t$, where X_f and X_i are the viable cell numbers at the beginning and at the end of any given time interval (Δt). The fold increase in total cell number was defined as the ratio between final and initial viable cell numbers for each passage. The cumulative fold increase was calculated as the product of fold increase values obtained for five consecutive passages.

Analysis of ground state, pluripotent stem cell expansion at clonal densities

Cells were seeded at low densities (400 cells/well) on gelatinized 24-well tissue culture plates and cultured for 6 days in *i*STEM serum-free medium either in 20% O_2 or 2% O_2 atmosphere. Medium was changed at Days 2 and 4. After 6 days, the colonies were counted and the diameter (in μm) of the colonies was measured. The efficiency in colony formation was defined as the ratio between the number of colonies formed and the number of cells seeded on a well (400 cells).

Proliferation analysis using PKH67 fluorescent dye

For cell division analysis using PKH67, cells were collected and stained with the dye according to the manufacturer's instructions (PKH67 green fluorescent cell linker kit for cell membrane labeling; Sigma). Since they are stably incorporated in the cell membrane, PKH67 molecules are equally distributed between daughter cells during cell division, and therefore each generation of cells is half as fluorescent as the previous one, allowing the determination of the number of cell divisions at any given time point in culture (da Silva et al., 2009). Between 100 000 and 1 000 000 cells were used for flow cytometry analysis (Day 0), and the remaining cells were plated with appropriate culture medium as described before. After 2 days in culture, cells were collected and the samples used for flow cytometry (FACSCalibur flow cytometer; Becton Dickinson). Proliferation analysis was performed using the CellQuest software and/or the Proliferation Wizard of ModFit software.

Cell cycle analysis using propidium iodine (PI) nucleic acid staining

Cells were collected and fixed in 2% (w/v) paraformaldehyde (Sigma) solution in PBS at room temperature for 20 min. After washing, cells were then incubated with 25 μg/mL RNase A (Roche) and stained with 5 μg/mL PI (BD) for 30 min at 37 °C in the dark. The acquisition of the samples was performed in a FACSCalibur flow cytometer and the data were analyzed using the ModFit software.

Neural commitment of mouse ES cells

After expansion, mouse ES cells were dissociated with Accutase, plated on gelatin-coated tissue culture plates, and incubated up to 8 days in RHB-A medium (Stem Cell Sciences Inc.), as described elsewhere (Diogo et al., 2008). Again, cells were maintained under atmospheric oxygen tension (20% O_2) or reduced oxygen atmosphere (2% O_2) during the neural commitment protocol. To quantify the population of Sox1-GFP$^+$ neural progenitors in each day, cells were recovered, counted, and analyzed by flow cytometry (Ying et al., 2003b). Settings were determined at the start of the experiment using undifferentiated 46C mouse ES cells as negative control.

Sox1$^+$ neural progenitors are nevertheless a transient population. Hence, to evaluate the influence of low oxygen tension on further neuronal differentiation, cells were collected at Day 6 of neural commitment and replated onto tissue culture plates precoated with polyornithine and laminin (30- to 60-min treatment with 0.01% (v/v) polyornithine solution in water, washing in PBS, and incubation for 2 h with 10 μg/mL laminin solution (both from Sigma) (Pollard et al., 2006)). Cells were maintained in culture in RHB-A medium for a period of time lower than 9 days with medium change every 3 days. Cells were analyzed for class III β-tubulin (TujI) expression at specific time points using flow cytometry.

Intracellular immunofluorescence staining for flow cytometry analysis

Cells were collected and fixed in 2% (w/v) paraformaldehyde (Sigma) solution in PBS. Cells were then permeabilized with 1% (w/v) saponin (Sigma) solution in PBS, followed by incubation in blocking solution (3% (v/v) normal goat serum (NGS; Sigma) in PBS) for 15 min. The primary antibody was added to the samples, and cells were incubated for 2 h at room temperature. Oct-4 and Nanog-expressing cells were evaluated by flow cytometry after intracellular staining using mouse monoclonal anti-Oct-3/4 (Chemicon), 1:30 (v/v) dilution in blocking solution, or rabbit polyclonal anti-Nanog (Santa Cruz Biotechnology), 1:500 (v/v) dilution in blocking solution, respectively. Neuronal differentiation efficiency was also assessed by flow cytometry with Alexa Fluor 488-labeled Neuronal Class III β-tubulin (Tuj1) (1:200 (v/v) dilution; Covance).

For Oct-4 and Nanog quantification, a secondary antibody (Alexa Fluor 488-conjugated goat-anti mouse and goat-anti rabbit IgG, respectively (Molecular Probes), 1:1000 dilution in blocking solution) was added to the cells after washing, followed by incubation for 45 min at room temperature. Cells incubated with appropriate secondary antibodies were used as negative controls. After washing, the acquisition of the samples was performed in a FACSCalibur flow cytometer and analyzed using the CellQuest software. Cell debris and dead cells were excluded from the analysis based on electronic gates using forward scatter (cell size) and side scatter (cell complexity) criteria. A minimum of 10 000 events was collected for each sample.

Real-time polymerase chain reaction

Quantitative real-time PCR was performed using previously established protocols (Abranches et al., 2006). Briefly, total RNA was isolated from $>10^6$ cells using the High Pure RNA Isolation Kit (Roche Diagnostics), and DNAse I (Roche) treatment according to the manufacturer's instructions. First-strand cDNA was synthesized using the Transcriptor First-Strand cDNA Synthesis Kit, also from Roche, and anchored-oligo$(dt)_{18}$. Real-time PCR was then performed on a Roche Light Cycler detection system, in a 20 μl final volume containing 2.0 mM $MgCl_2$ solution, 0.2 μM of each primer, 4.0 μl of sample, and SYBR Green I mixture. Threshold cycle (C_T) values were calculated using the LightCycler software 3.4 (Roche) and the Fit Points method. *Gapdh* was used as control housekeeping gene in real-time PCR experiments. Relative quantification of gene expression was performed using the delta-delta threshold cycle method ($\Delta\Delta C_T$). The primer sequences used to assess gene expression can be seen in Table S1 (Supplementary Data).

Metabolite analysis

Metabolite analysis was performed as previously described (Fernandes et al., 2010). Briefly, the exhausted medium was recovered after cell culture and samples were centrifuged for 10 min at 1500 rpm to remove dead cells and debris. The supernatants were then collected and kept frozen until analysis. Fresh medium was also analyzed and the results were used for the determination of consumption and production rates. Glucose, lactate, glutamine, and ammonia concentrations were measured using a multiparameter analyzer (YSI 7100MBS; Yellow Springs Instruments). The specific metabolic rates (q_{Met}, pmol/(cell. day)) were calculated for every time interval using the following equation: $q_{Met} = \Delta Met/(\Delta t.\Delta X_v)$, where ΔMet is the variation in metabolite concentration during the time period Δt and ΔX_v the logarithmic mean of viable cell number during the same period. The apparent lactate from glucose yield ($Y'_{lactate/glucose}$) was calculated as the ratio between $q_{lactate}$ and $q_{glucose}$, and the apparent ammonia from glutamine yield ($Y'_{ammonia/glutamine}$) was also determined as the ratio between $q_{ammonia}$ and $q_{glutamine}$. Cell yields from glucose and glutamine were also calculated as the ratio between μ and $q_{glucose}$ or $q_{glutamine}$, respectively.

Statistical analysis

Statistical analysis was performed using the SPSS 16.0 software (SPSS Inc., Chicago, IL, http://www.spss.com.uk).

The nonparametric Wilcoxon–Mann–Whitney test was used to evaluate statistical significance of two independent samples ($P<0.05$). Unless otherwise stated, error bars represent the standard error of the mean (SEM) from triplicates for each condition.

Acknowledgments

T.G.F. and A.M.P acknowledge support from Fundação para a Ciência e a Tecnologia, Portugal (SFRH/BD/24365/2005 and SFRH/BD/36070/2007, respectively). This work was financially supported by Fundação para a Ciência e a Tecnologia, through the MIT-Portugal Program, Bioengineering Systems Focus Area. The authors gratefully acknowledge Domingos Henrique (Institute of Molecular Medicine, Lisboa, Portugal) for providing the E14tg2a and the 46C mouse embryonic stem cell lines, and HEK-293 cells for production of human LIF.

Appendix A. Supplementary data

Supplementary data for this article may be found in the online version at doi:10.1016/j.scr.2010.04.003.

References

Abranches, E., O'Neill, A., Robertson, M.J., Schaffer, D.V., Cabral, J.M.S., 2006. Development of quantitative PCR methods to analyse neural progenitor cell culture state. Biotechnol. Appl. Biochem. 44, 1–8.

Burdon, T., Smith, A., Savatier, P., 2002. Signalling, cell cycle and pluripotency in embryonic stem cells. Trends Cell Biol. 12, 432–438.

Covello, K.L., Kehler, J., Yu, H., Gordan, J.D., Arsham, A.M., Hu, C.J., Labosky, P.A., Simon, M.C., Keith, B., 2006. HIF-2alpha regulates Oct-4: effects of hypoxia on stem cell function, embryonic development, and tumor growth. Genes Dev. 20, 557–570.

da Silva, C.L., Gonçalves, R., Porada, C.D., Ascensão, J.L., Zanjani, E.D., Cabral, J.M.S., Almeida-Porada, G., 2009. Differences amid bone marrow and cord blood hematopoietic stem/progenitor cell division kinetics. J. Cell. Physiol. 220, 102–111.

Diogo, M.M., Henrique, D., Cabral, J.M.S., 2008. Optimization and neural commitment of mouse embryonic stem cells. Biotechnol. Appl. Biochem. 49, 105–112.

Doble, B.W., Woodgett, J.R., 2003. GSK-3: tricks of the trade for a multi-tasking kinase. J. Cell Sci. 116, 1175–1186.

Duval, D., Malaisé, M., Reinhardt, B., Kedinger, C., Boeuf, H., 2004. A p38 inhibitor allows to dissociate differentiation and apoptotic processes triggered upon LIF withdrawal in mouse embryonic stem cells. Cell Death Differ. 11, 331–341.

Fernandes, T.G., Fernandes-Platzgummer, A.M., da Silva, C.L., Diogo, M.M., Cabral, J.M.S., 2010. Kinetic and metabolic analysis of mouse embryonic stem cell expansion under serum-free conditions. Biotechnol. Lett. 32, 171–179.

Follmar, K.E., Decroos, F.C., Prichard, H.L., Wang, H.T., Erdmann, D., Olbrich, K.C., 2006. Effects of glutamine, glucose, and oxygen concentration on the metabolism and proliferation of rabbit adipose-derived stem cells. Tissue Eng. 12, 3525–3533.

Hanna, J., Markoulaki, S., Mitalipova, M., Cheng, A.W., Cassady, J. P., Staerk, J., Carey, B.W., Lengner, C.J., Foreman, R., Love, J., et al., 2009. Metastable pluripotent states in NOD-mouse-derived ESCs. Cell Stem Cell 4, 513–524.

Ivanovic, Z., 2009. Hypoxia or in situ normoxia: the stem cell paradigm. J. Cell. Physiol. 219, 271–275.

Jauniaux, E., Gulbis, B., Burton, G.J., 2003. Physiological implications of the materno-fetal oxygen gradient in human early pregnancy. Reprod. Biomed. Online 7, 250–253.

Jeong, C.H., Lee, H.J., Cha, J.H., Kim, J.H., Kim, K.R., Kim, J.H., Yoon, D.K., Kim, K.W., 2007. Hypoxia-inducible factor-1 alpha inhibits self-renewal of mouse embryonic stem cells in vitro via negative regulation of the leukemia inhibitory factor-STAT3 pathway. J. Biol. Chem. 282, 13672–13679.

Kirouac, D.C., Zandstra, P.W., 2008. The systematic production of cells for cell therapies. Cell Stem Cell 3, 369–381.

Klimanskaya, I., Rosenthal, N., Lanza, R., 2008. Derive and conquer: sourcing and differentiating stem cells for therapeutic applications. Nat. Rev. Drug Discov. 7, 131–142.

Krishnamoorthy, M., Heimburg-Molinaro, J., Bargo, A.M., Nash, R.J., Nash, R.J., 2009. Heparin binding epidermal growth factor-like growth factor and PD169316 prevent apoptosis in mouse embryonic stem cells. J. Biochem. 145, 177–184.

Kurosawa, H., Kimura, M., Noda, T., Amano, Y., 2006. Effect of oxygen on in vitro differentiation of mouse embryonic stem cells. J. Biosci. Bioeng. 101, 26–30.

Lee, Y.M., Jeong, C.H., Koo, S.Y., Son, M.J., Song, H.S., Bae, S.K., Raleigh, J.A., Chung, H.Y., Yoo, M.A., Kim, K.W., 2001. Determination of hypoxic region by hypoxia marker in developing mouse embryos in vivo: a possible signal for vessel development. Dev. Dyn. 220, 175–186.

Morrison, S.J., Csete, M., Groves, A.K., Melega, W., Wold, B., Anderson, D.J., 2000. Culture in reduced levels of oxygen promotes clonogenic sympathoadrenal differentiation by isolated neural crest stem cells. J. Neurosci. 20, 7370–7376.

Mottet, D., Dumont, V., Deccache, Y., Demazy, C., Ninane, N., Raes, M., Michiels, C., 2003. Regulation of hypoxia-inducible factor-1alpha protein level during hypoxic conditions by the phosphatidylinositol 3-kinase/Akt/glycogen synthase kinase 3beta pathway in HepG2 cells. J. Biol. Chem. 278, 31277–31285.

Nichols, J., Smith, A., 2009. Naive and primed pluripotent states. Cell Stem Cell 4, 487–492.

Niwa, H., Burdon, T., Chambers, I., Smith, A., 1998. Self-renewal of pluripotent embryonic stem cells is mediated via activation of STAT3. Genes Dev. 12, 2048–2060.

Ozturk, S.S., Riley, M.R., Palsson, B.O., 1992. Effects of ammonia and lactate on hybridoma growth, metabolism, and antibody production. Biotechnol. Bioeng. 39, 418–431.

Pistollato, F., Chen, H.L., Schwartz, P.H., Basso, G., Panchision, D.M., 2007. Oxygen tension controls the expansion of human CNS precursors and the generation of astrocytes and oligodendrocytes. Mol. Cell. Neurosci. 35, 424–435.

Pollard, S.M., Conti, L., Sun, Y., Goffredo, D., Smith, A., 2006. Adherent neural stem (NS) cells from fetal and adult forebrain. Cereb. Cortex 16 (Suppl. 1), i112–i120.

Pouton, C.W., Haynes, J.M., 2005. Pharmaceutical applications of embryonic stem cells. Adv. Drug Deliv. Rev. 57, 1918–1934.

Powers, D.E., Millman, J.R., Huang, R.B., Colton, C.K., 2008. Effects of oxygen on mouse embryonic stem cell growth, phenotype retention, and cellular energetics. Biotechnol. Bioeng. 101, 241–254.

Reitzer, L.J., Wice, B.M., Kennel, D., 1979. Evidence that glutamine, not sugar, is the major energy source for cultured HeLa cells. J. Biol. Chem. 254, 2669–2676.

Rodesch, F., Simon, P., Donner, C., Jauniaux, E., 1992. Oxygen measurements in endometrial and trophoblastic tissues during early pregnancy. Obstet. Gynecol. 80, 283–285.

Sato, N., Meijer, L., Skaltsounis, L., Greengard, P., Brivanlou, A.H., 2004. Maintenance of pluripotency in human and mouse embryonic stem cells through activation of Wnt signaling by a pharmacological GSK-3-specific inhibitor. Nat. Med. 10, 55–63.

Schop, D., Janssen, F.W., van Rijn, L.D., Fernandes, H., Bloem, R.M., de Bruijn, J.D., van Dijkhuizen-Radersma, R., 2009. Growth, metabolism, and growth inhibitors of mesenchymal stem cells. Tissue Eng. A 15, 1877–1886.

Silva, J., Smith, A., 2008. Capturing pluripotency. Cell 132, 532–536.
Smith, A.G., 2001. Embryo-derived stem cells: of mice and men. Annu. Rev. Cell Dev. Biol. 17, 435–462.
Sutter, D.M., Krause, K.-H., 2008. Neural commitment of embryonic stem cells: molecules, pathways and potential for cell therapy. J. Pathol. 215, 355–368.
Vriezen, N., Romein, B., Luyben, K.C., van Dijken, J.P., 1997. Effects of glutamine supply on growth and metabolism of mammalian cells in chemostat culture. Biotechnol. Bioeng. 54, 272–286.
Watanabe, K., Ueno, M., Kamiya, D., Nishiyama, A., Matsumura, M., Wataya, T., Takahashi, J.B., Nishikawa, S., Nishikawa, S., Muguruma, K., et al., 2007. A ROCK inhibitor permits survival of dissociated human embryonic stem cells. Nat. Biotechnol. 25, 681–686.
Ying, Q.-L., Nichols, J., Chambers, I., Smith, A., 2003a. BMP induction of Id proteins suppresses differentiation and sustains embryonic stem cell self-renewal in collaboration with STAT3. Cell 115, 281–292.
Ying, Q.-L., Stavridis, M., Griffiths, D., Li, M., Smith, A., 2003b. Conversion of embryonic stem cells into neuroectodermal precursors in adherent monoculture. Nat. Biotechnol. 21, 183–186.
Ying, Q.-L., Wray, J., Nichols, J., Batlle-Morera, L., Doble, B., Woodgett, J., Cohen, P., Smith, A., 2008. The ground state of embryonic stem cell self-renewal. Nature 453, 519–523.